THE JOURNAL OF PHYSICAL CHEMISTRY A

Article

pubs.acs.org/JPCA

Infrared Signature of the Early Stage Microsolvation in the $NaSO_4^-(H_2O)_{1-5}$ Clusters: A Simulation Study

Tan Jin,[†,‡,#] BingBing Zhang,[‡,§,#] Jian Song,[∥] Ling Jiang,*[,‡] Yishen Qiu,*[,†] and Wei Zhuang*[,‡]

[†]College of Photonic and Electronic Engineering, Fujian Normal University, Fuzhou 350007, Fujian, People's Republic of China

[‡]State Key Laboratory of Molecular Reaction Dynamics, Dalian Institute of Chemical Physics, Chinese Academy of Sciences, Dalian 116023, Liaoning, People's Republic of China

[§]College of Chemistry and Molecular Engineering, Zhengzhou University, Zhengzhou 450001, Henan, People's Republic of China

[∥]Department of Physics, Henan Normal University, Xinxiang 453007, Henan, People's Republic of China

Supporting Information

ABSTRACT: Infrared photon dissociation (IRPD) spectra of the $NaSO_4^-(H_2O)_n$ clusters with up to five water molecules have been studied using quantum chemical calculations. Our calculation reveals that the splitting of the peaks in the ~800−1300 cm^{-1} region of the IRPD spectra, which contains the information on S−O bond stretching of the anion, indicates the deviation of the cation from the C_{3v} axis as well as the asymmetric distribution of the water molecules. The frequency of the H-bonded O−H stretching peak in the ~2300−3000 cm^{-1} window, on the other hand, provides information on the position of the newly added water molecule with respect to the cation. The IRPD technique thus provides abundant structural information on the early stage of the microsolvation and has the potential to become a powerful tool complementary to photoelectron spectroscopy.

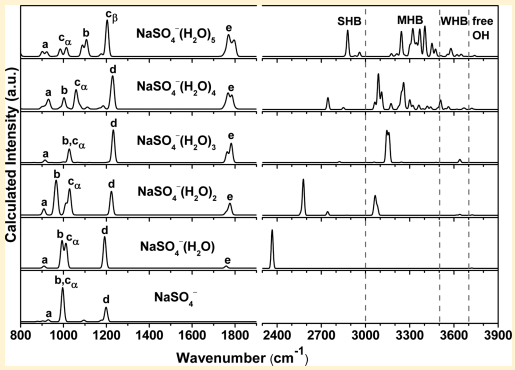

INTRODUCTION

Dissociation of the salts in water is a fundamental phenomenon in nature. When the water is absent, the electrostatic interaction between the anion and the cation causes them to associate with each other and form the contact ion pairs (CIPs).[1] During the solvation process, the ions with opposite charges can be separated by the water molecules to form solvent-separated ion pairs (SSIPs).[2] Despite intensive efforts from both experimental and theoretical aspects to elaborate on how the simple salt molecules dissolve in the aqueous solutions, there are still quite a few issues about this process that are not very well understood. One interesting question, for instance, is what will be the smallest number of water molecules needed to separate the CIP of a certain salt (so-called "microsolvation" issue). Obviously, the study on microsolvation bears significant importance in the atmospheric and oceanic chemical cycle.[3−6]

Different experimental techniques[7−11] have been developed to investigate the microsolvated clusters of certain ion pairs in the gas phase. Because the electronic state of a SSIP would be different from that of a CIP, anion photoelectron spectroscopy (PES),[8,12−17] which probes the change of salt electronic state, has been applied to study the microsolvation. Wang and co-workers have investigated the dissolution of $NaSO_4^-(H_2O)_n$ with up to four water molecules using this technique combined with quantum chemical calculations.[18] The calculation suggests that the first three water molecules form a solvation ring structure between the ion pair, while the fourth water binds to the sulfate anion and stays farther away from the sodium cation. The calculated electron binding energy of the sulfate anion has successive increments as the response to the increasing number of water molecules, which plausibly agrees with the experimental measurements and provides justification to the calculated microsolvation structures.

A recently emerging category of tools for the structural characterization of ion−water clusters in the gas phase is infrared photon dissociation (IRPD) spectroscopy.[19−29] Under readily achievable experimental conditions, absorption of single or multiple IR photons by a hydrated ion can induce a measurable increase in the fragment, resulting in IRPD spectra that closely resemble linear absorption spectra. Compared with the conventional vibrational spectroscopy in the bulk solution phase, IRPD spectroscopy has the advantage that any competing effects of the ions other than the pair under investigation can be eliminated.

Two frequency windows, ~800−2000 and ~2300−4000 cm^{-1}, are commonly employed in IRPD spectra for the ion−water cluster investigation, within which the former indicates the influence of the hydration on the structure of the ionic core

Special Issue: International Conference on Theoretical and High Performance Computational Chemistry Symposium

Received: March 21, 2014
Revised: May 30, 2014
Published: May 30, 2014

   dx.doi.org/10.1021/jp5028299 | J. Phys. Chem. A 2014, 118, 9157−9162

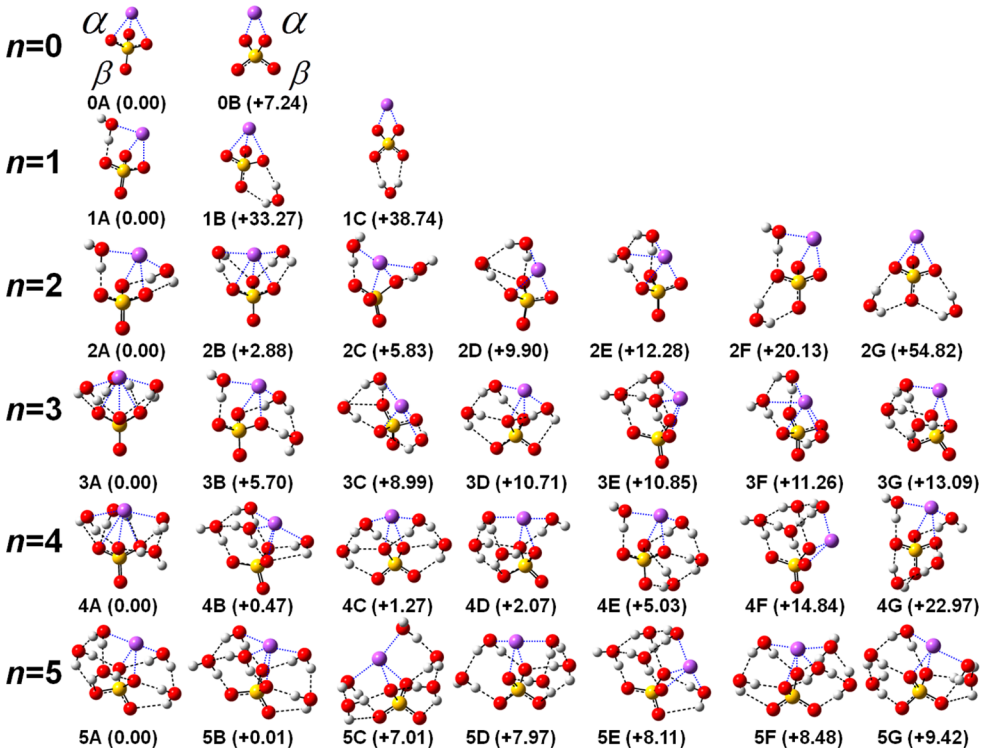

Figure 1. Optimized structures of the $(NaSO_4)^-(H_2O)_n$ (n = 0−5) clusters (Na, purple; S, yellow; O, red; H, gray). Relative energies are given in kJ/mol.

with respect to their stretching modes while the latter contains information about the solvent network with respect to O−H stretching modes. Recently, Jiang and co-workers[30] investigated the 3000−3800 cm^{-1} region of $[MgNO_3(H_2O)_{1-4}]^+$ clusters using a Herriott-type multipass cell and found that the first four water molecules only weakly perturb the ionic bond in this prototypical salt, and no hint of the ion separation is observed. This is probably due to the rather strong interaction between the cation and anion in these systems.

In the current work, we carried out theoretical modeling of IRPD spectra of $NaSO_4^-(H_2O)_n$ clusters with up to five water molecules in both the sulfate-stretch region and the hydrogen-stretch region. Our calculation indicates that, consistent with the previous report,[18] when adding up to five water molecules, the ion pair goes through the early stage of microsolvation. IR spectroscopic modeling reveals that the splitting of peaks in the range of 800−1300 cm^{-1}, which is related to the S−O stretchings in the anion core, provides information on how the cluster configuration deviates from the C_{3v} symmetry. Furthermore, the blue shift of the peak in the 2300−3000 cm^{-1} region provides information on the position of the newly added water molecule related to the cation. Our simulation thus suggests that the IRPD technique can be used as an informative probe for microsolvation complementary to the PES measurement.

This paper is organized as follows. In the Theoretical Methods section, the simulation protocol is described in detail. The simulation results are demonstrated in the results section, followed by the discussion.

■ THEORETICAL METHODS

Quantum chemical calculations were carried out using the Gaussian 09 suite of programs. Initial configurations were built on the basis of chemical intuition and the relevant structures of the hydrated clusters reported in the literature.[7−31] Geometry optimizations were performed using B3LYP/6-31+G(d) without any symmetry restriction. To obtain more accurate energy changes, the 10 lowest structures of each cluster size were further optimized at the MP2/aug-cc-pVDZ level. Tight convergence of the optimization and the self-consistent field procedures were utilized. Harmonic vibrational frequencies of optimized structures were calculated using MP2/aug-cc-pVDZ, and zero-point energy corrections were considered. MP2/aug-cc-pVTZ and CCSD(T)/aug-cc-pVDZ calculations were carried out for n = 1 to assess the uncertainty related to the choice of computational methods, and the relative energies observed were in accord with the MP2/aug-cc-pVDZ ones (Table S1, Supporting Information). Vibrational frequencies below 2000 cm^{-1} were scaled by 1.0418, and those in the 2000−4000 cm^{-1} region were scaled by 0.9615. This set of scaling factors lies in the middle of the range of scaling factors used in comparable studies.[31−34] The resulting IR stick spectra were convoluted by a Gaussian line shape function with a width of 15 cm^{-1} (fwhm).

To explore the physical origin of IR spectral features, we carried out the first-order vibrational transitional density cubes (VTDCs) analysis[35,36] on typical modes. VTDC describes how the electron density of a molecule changes with respect to its vibrational motion. The first-order VTDC for mode k on a molecule was calculated as

$$\frac{\partial P}{\partial Q_k} = \frac{P(\delta Q_k) - P(-\delta Q_k)}{2\delta Q_k} \quad (1)$$

Here, P is the electronic density cube, and Q_k is the normal coordinate of mode k. First, the ground-state equilibrium structure of the molecule was optimized, and normal mode coordinates were analyzed. Then, a small step $\delta Q_k(-\delta Q_k)$ of

vibration along the (opposite) mode Q_k was added to the equilibrium geometry, and the electron density cube $P(\delta Q_k)$-$(P(-\delta Q_k))$ at this geometry was generated. Finally, the VTDC was obtained using eq 1. The vibrational step was 0.01 Å.

RESULTS AND DISCUSSION

Configurations of the $NaSO_4^-(H_2O)_n$ Clusters. Several representative low-lying structures of the $NaSO_4^-(H_2O)_n$ (n = 0−5) clusters are presented in Figure 1. The structures are labeled according to the number of water molecules and relative energies. For each number of water molecules, the populations (Table 1) of the seven lowest-energy cluster configurations were calculated on the basis of the free-energy change (ΔG) at 298.15 K and 1 atm following the Boltzmann distribution. Detailed discussion of cluster configurations at different cluster sizes is given in the Supporting Information. For n = 0−5, the most stable configurations have dominating populations. We therefore, unless pointed out specifically, mainly analyze the IR features by looking at the most stable structures.

Table 1. ΔG and Weighted Factors of $NaSO_4^-(H_2O)_n$ (n = 0−5)

isomers	ΔG(kJ/mol)	population at 298.15 K and 1 atm
0A	0.00	0.903
0B	5.54	0.097
1A	0.00	1.000
1B	28.68	0.000
1C	32.38	0.000
2A	0.00	0.634
2B	1.88	0.297
2C	5.76	0.062
2D	12.64	0.004
2E	13.03	0.003
2F	17.02	0.001
2G	46.93	0.000
3A	0.00	0.969
3B	9.79	0.019
3C	12.82	0.005
3D	15.71	0.002
3E	17.37	0.001
3F	13.96	0.003
3G	18.11	0.001
4A	0.00	0.607
4B	3.21	0.166
4C	5.46	0.067
4D	3.77	0.133
4E	7.73	0.027
4F	20.39	0.000
4G	19.04	0.000
5A	0.00	0.538
5B	1.25	0.325
5C	5.79	0.052
5D	6.19	0.044
5E	9.42	0.012
5F	9.41	0.012
5G	8.59	0.017

As the number of water molecules increases, the $Na^+-SO_4^{2-}$ pair configuration gradually changes. With up to five water molecules, although the ion pair configuration is still far from a complete SSIP, obvious deviation from the tridentate CIP configuration of Na^+-SO_4^{2-} can already be observed. In the following, we briefly describe several typical features of the solvation processes.

The Na−S distances in the most stable structures for the n = 0−5 clusters are 2.50, 2.71, 2.81, 2.84, 2.93, and 2.99 Å (Figure S1, Supporting Information), respectively. The values of the Na−S distances for all isomers are displayed in Table S2 (Supporting Information). The cation and anion thus depart gradually from each other when adding more water molecules, which is consistent with the previous study.[18]

We can define two types of sulfate oxygen atoms in the clusters, one that faces the Na^+ ion (α-O) and the other that does not (β-O). Figure 1 indicates that the water molecules prefer to occupy the α-O binding sites of the sulfate ion (thus stay between the cation and anion) in the n = 1−3 clusters and only start to fill the β-O binding sites at n = 4. In the n = 5 clusters, interestingly, a bidentately bound configuration is more preferred. To quantify this trend, we define the shift angle θ in Figure 2, which quantifies how the sodium cation deviates from the C_{3v} axis. The values of θ for all isomers are shown in Table S3 (Supporting Information). The weighted shift angles are 5.5, 22.3, 17.6, 0.9, 24.6, and 45.2° from n = 0 to 5, respectively.

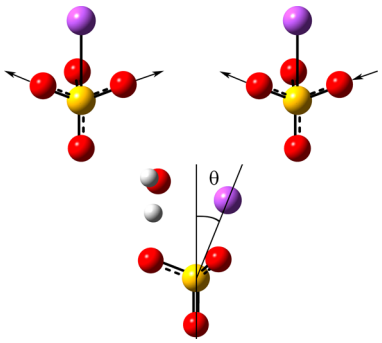

Figure 2. The top half is the sketch map about S−O_2 symmetrical stretching (left) and S−O_2 antisymmetrical stretching (right). The black arrows stand for the direction of vibration. The bottom half is the schematic diagram about the shift angle θ.

Another marker for the microsolvation process is the position of the water molecule with free OH. Because the first three water molecules prefer to stay in between the cation and anion and occupy the α-O binding sites of sulfate, the water molecule with free OH stays next to the cation ion at n = 1 or 2. At n = 3, a stable three-water microhydration layer forms between the ion pair, and none of these water molecules have a free OH. At n = 4 and 5, the water with free OH appears at the β-O position, which is separated from the cation by the network of three water layers. The position of the water molecule with free OH thus provides concerted information on how the ion pair is hydrated.

Recent PES and quantum chemical studies on the $NaBO_2^-(H_2O)_n$ clusters indicated that the transition from the CIP structure to the SSIP structure in these clusters starts at n = 3.[16] Very recently, Li et al. investigated the microsolvation of LiI and CsI in water and found that the SSIP types of structures start to appear at n = 3 in $LiI(H_2O)_n^-$ cluster anions and at n = 5 in neutral $LiI(H_2O)_n$, whereas no obvious evidence was observed toward the formation of SSIP structure in the $CsI(H_2O)_n$ clusters.[17]

IR Spectra. The simulated IRPD spectra for each of the representative structures with n = 0−5 are presented in Figures S2−S7 (Supporting Information). Detailed assignments are summarized in Table S4−S36 (Supporting Information). The overall signal (Figure 3) is calculated as the population weighted average of the contributions from the representative structures.

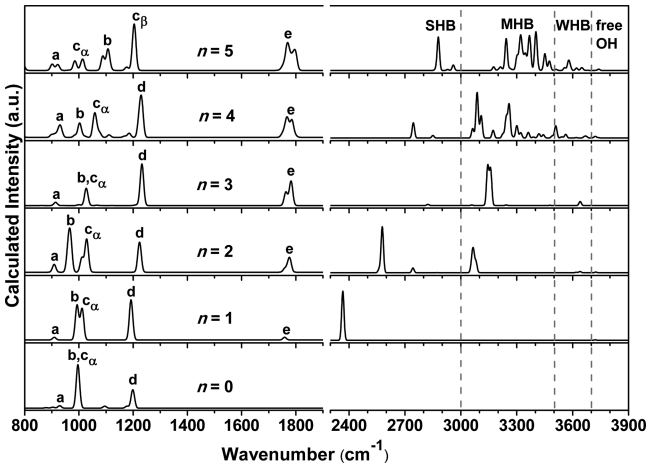

Figure 3. Weighted scaled IR spectra of $NaSO_4^-(H_2O)_n$(n = 0−5). The label a stands for S−O_4 stretching, b for symmetric S−O_2 stretching, c_α for antisymmetric S−O_2 stretching involving α-O atoms, c_β for antisymmetric S−O_2 stretching involving β-O atoms, d for S═O stretching involving β-O atoms, e for water bending, SHB for O−H stretching for a strong H-bond, MHB for O−H stretching for a medium H-bond, WHB for O−H stretching for a weak H-bond, and free OH for free O−H stretching in the water molecule.

Two spectral features are found to be highly interesting in the overall signals. The first one is the splitting of S−O bond stretching peak (around 1000 cm^{-1}), and the second one is the blue shift of O−H stretching below 3000 cm^{-1}.

The 800−1300 cm^{-1} region in the total IR spectra (Figure 3) is displayed, in which the peaks are related to the stretching of the sulfate. Two important normal modes of the S−O_2 symmetrical stretching (label b) and S−O_2 antisymmetrical stretching involving α-O (label c_α) are schematically shown in Figure 3. An increasing splitting between b and c_α peaks, $\Delta = |\omega_b - \omega_{c_\alpha}|$, can be clearly observed in Figure 3. When n changes from 0 to 2, the value of Δ rises from 0, to ∼20, to ∼60 cm^{-1}. At n = 3, the splitting between peaks b and c_α disappears. For n = 4 and 5, Δ increases again to ∼55 and ∼100 cm^{-1}.

The 2300−3800 cm^{-1} region in the total IR spectra (Figure 3) gives the information on the O−H stretches. The peaks in the 2300−3000 cm^{-1} region, which are related to the H-bonded O−H stretching of a dangling water molecule, systematically have the blue shift with the increase of water molecules. The frequency for this peak with n = 1, 2, 4, and 5 are 2365.7, 2577.2, 2744.0, and 2878.0 cm^{-1}, respectively, while there is no peak for n = 3.

In the following, we discuss in detail how the microsolvation is reflected in these spectral features.

Sulfate-Stretch Regime. In the 800−1300 cm^{-1} region (Figure 3), the splitting between peaks b and c_α increases from 0 to ∼20 and ∼60 cm^{-1} for n = 0−2, disappears at n = 3, and recovers to be ∼55 and ∼100 cm^{-1} for n = 4 and 5, respectively. To study the origin of such splitting, we calculated the VTDCs of these two modes for the most stable configurations in n = 0−5 (Figure 4). VTDC indicates the contributions to the vibration from different areas of the cluster.

For **0A**, due to the C_{3v} symmetry of the cluster structure, VTDCs of b and c_α modes are rotationally symmetrical with each other. Because the components of these two modes in the cluster give almost the same contribution, these two degenerate modes are predicted to have the same frequency (Table S4, Supporting Information). At n = 1 and 2, the structural symmetry is broken, and the sodium cation is pressed away from the C_{3v} axis (∼22°). Meanwhile, the VTDCs have increasing contribution from the asymmetrically distributed water molecules. Thus, the VTDCs of these two modes deviate from the C_{3v} symmetry and become more and more different from each other, resulting in the increase of the splitting. At n = 3, the C_{3v} symmetry recovers due to the formation of the three

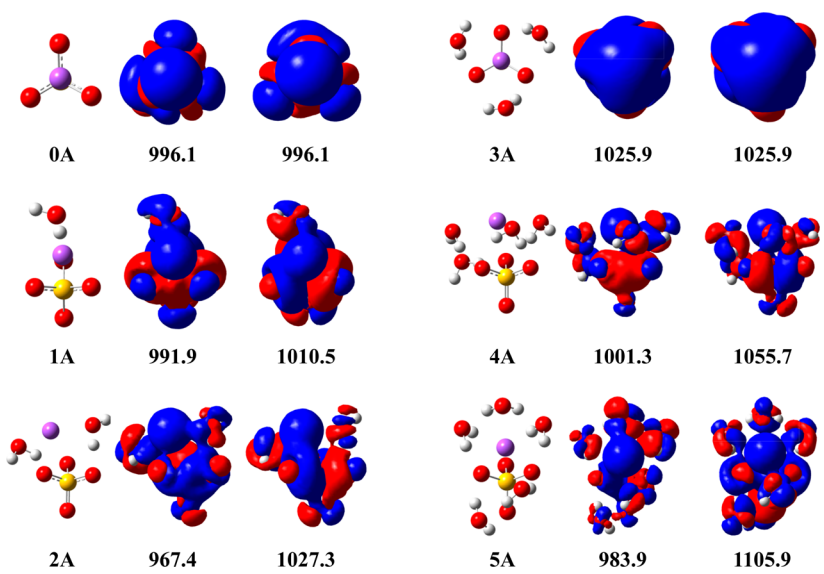

Figure 4. VTDCs of S−O_2 stretching modes for the most stable isomer in each cluster. The absolute isovalue is 0.0057 au. The red color stands for positive VTDCs and blue for negative VTDCs.

water molecule solvation ring structure. The VTDCs of the two modes again become almost identical, which eliminates the splitting between the b and c_α peaks. At $n = 4$, the cation only lightly deviates from the C_3 axis (~14°), but a fourth water molecule appears at the β-O binding sites. The VTDCs deviate from the C_{3v} symmetry and become different from each other again, which causes the splitting. At $n = 5$, the cation has a very significant deviation from the C_3 axis (48.5°), and the splitting further enlarges to be 100 (Figure 3).

Hydrogen-Stretch Regime. The peaks in the 2300−3000 cm^{-1} region of the average IR spectra (Figure 3) for $NaSO_4^-(H_2O)_n$ (n = 1−5) are related to the H-bonded O−H stretching of a dangling water. These peaks are blue-shifted with the increase of the number of water molecules. In the following, we again examine the most stable configurations with a free OH in n = 1−5 (Figure 1) and attempt to give a qualitative discussion on the origin of this blue shift.

In all of the cluster conformers, the water molecule with the free OH stays next to one oxygen of the sulfate anion, but their relative configuration with the sodium cation is different. At n = 1, the sodium cation stays next to the water oxygen, which attracts the electron in the oxygen and hydrogen and induces a strong red shift of the H-bonded O−H stretching frequency. At n = 2, a second water molecule appears next to the sodium, which weakens the capability of the cation to attract the electron from the water molecule with free OH; thus, the frequency is blue-shifted as compared to n = 1. At n = 3, the three-water hydration ring forms in the most stable structure; thus, no free OH is observed. At n = 4, the largest contribution comes from **4B**, and that from **4A** is negligible. The water with free OH appears at the position farther away from sodium with two water molecules in between. The frequency of H-bonded OH is thus further blue-shifted as compared to n = 2. At n = 5, the most stable structure does not have a free OH. However, the 5B structure, with the second largest population (32.5%), has a free OH water that is even farther away from the sodium, inducing a larger blue shift. Note that **5B** is calculated to be higher in energy only by +0.01 kJ/mol than **5A** (Figure 1).

The blue shift of the H-bonded O−H stretching frequency in the 2300−3000 cm^{-1} region thus directly reflects the extent that the cluster is hydrated. When there is only one water molecule, the ion pair is least hydrated, and the water molecule stays next to the cation. The attraction from the cation causes a significant red shift of the H-bonded O−H stretching frequency with respect to the free water molecule. A stable network of the three-water ring is formed at n = 3. The attraction from the cation on the water with free OH is weakened and later screened by the hydration ring. This is reflected on the frequency of the H-bonded OH vibration with free OH as a monotonic blue shift. As listed in Table 2, the NBO charge of H-bonded hydrogen atom in the water molecule decreases from 0.565 to 0.560 with the increase of hydrated cluster size, indicating the weakening trend of the H-bonds, which is consistent with the blue shift of the H-bonded O−H stretching frequency.

Table 2. NBO Charge Distribution of the Most Stable Structures with a Free OH

isomers	Na	S	$O_{H\text{-}bond}$	O_{water}	$H_{H\text{-}bond}$	H_{free}
1A	0.918	2.752	−1.144	−1.102	0.565	0.472
2A	0.894	2.760	−1.137	−1.086	0.563	0.476
3A				(no free OH)		
4B	0.872	2.780	−1.142	−1.084	0.562	0.482
5B	0.876	2.784	−1.128	−1.077	0.560	0.483

CONCLUSIONS

In summary, our modeling of the IR spectra of the $NaSO_4^-(H_2O)_n$ ion pairs with up to five water molecules suggests that the IRPD technique could provide abundant structural information on the early stage of the microsolvation of this ion pair.

The splitting of the b and c_α peaks in the range of 800−1300 cm^{-1}, which is related to the S−O bond stretchings in the anion core, provides information on how the cluster configuration deviates from the C_{3v} symmetry. This deviation is caused by the fact that the cation is pushed away from the C_{3v} axis, as well as the asymmetric distribution of the water molecules, which are both the direct reflection of the formation of the hydration shell. Interestingly, the blue shift of the strong H-bonds in the 2300−3000 cm^{-1} region with the increase of water molecules provides concerted information on the position of the newly added water molecule related to the cation, which is again a structure marker of the microhydration. The IRPD technique, combined with theoretical modeling, thus can provide a vivid physical picture about how the water molecules microhydrate and separate the $Na^+-SO_4^{2-}$ ion pair in the early stage of the microsolvation.

ASSOCIATED CONTENT

Supporting Information

Figure S1: The distance in between the Na and S atoms for the most stable isomer. Figures S2−S7: The simulated IR spectra for representative configurations for n = 0−5. Table S1: Comparison in the relative energy at MP2/aug-cc-pvdz, MP2/aug-cc-pvtz, and CCSD(T)/aug-cc-pVDZ for $NaSO_4^-(H_2O)$ isomers. Table S2: The distance and the weighted one in between the Na and S atoms for representative low-lying structures. Table S3: The shift angle θ for representative low-lying isomers. Tables S4−S36: Scaled MP2/aug-cc-pvdz harmonic frequencies for the isomers shown in Figure 1. This material is available free of charge via the Internet at http://pubs.acs.org.

AUTHOR INFORMATION

Corresponding Authors

*E-mail: ljiang@dicp.ac.cn. Tel: +86-411-84379857 (L.J.).
*E-mail: ysqiu@fjnu.edu.cn. Tel: +86-591-22868152 (Y.Q.).
*E-mail: wzhuang@dicp.ac.cn. Tel: +86-411-84379627 (W.Z.).

Author Contributions

#T.J. and B.B.Z. contributed equally to this work.

Notes

The authors declare no competing financial interest.

ACKNOWLEDGMENTS

This work is supported by the National Natural Science Foundation of China (Grants 21103166, 21273232, and 21327901) and the Ministry of Science and Technology of China (Grant 2011YQ09000505). L.J. acknowledges the Hundred Talents Program of Chinese Academy of Sciences.

REFERENCES

(1) Blandamer, M. J.; Fox, M. F. Theory and Applications of Charge-Transfer-to-Solvent Spectra. *Chem. Rev.* **1970**, *70*, 59−93.

(2) Jungwirth, P. How Many Waters Are Necessary to Dissolve a Rock Salt Molecule? *J. Phys. Chem. A* **1999**, *104*, 145−148.
(3) Gard, E. E.; Kleeman, M. J.; Gross, D. S.; Hughes, L. S.; Allen, J. O.; Morrical, B. D.; Fergenson, D. P.; Dienes, T.; E. Gälli, M.; Johnson, R. J.; Cass, G. R.; Prather, K. A. Direct Observation of Heterogeneous Chemistry in the Atmosphere. *Science* **1998**, *279*, 1184−1187.
(4) Oum, K. W.; Lakin, M. J.; DeHaan, D. O.; Brauers, T.; Finlayson-Pitts, B. J. Formation of Molecular Chlorine from the Photolysis of Ozone and Aqueous Sea-Salt Particles. *Science* **1998**, *279*, 74−76.
(5) Knipping, E. M.; Lakin, M. J.; Foster, K. L.; Jungwirth, P.; Tobias, D. J.; Gerber, R. B.; Dabdub, D.; Finlayson-Pitts, B. J. Experiments and Simulations of Ion-Enhanced Interfacial Chemistry on Aqueous NaCl Aerosols. *Science* **2000**, *288*, 301−306.
(6) Finlayson-Pitts, B. J. The Tropospheric Chemistry of Sea Salt: A Molecular-Level View of the Chemistry of NaCl and NaBr. *Chem. Rev.* **2003**, *103*, 4801−4822.
(7) Ault, B. S. Infrared Spectra of Argon Matrix-Isolated Alkali Halide Salt/Water Complexes. *J. Am. Chem. Soc.* **1978**, *100*, 2426−2433.
(8) Wang, X.-B.; Ding, C.-F.; Nicholas, J. B.; Dixon, D. A.; Wang, L.-S. Investigation of Free Singly and Doubly Charged Alkali Metal Sulfate Ion Pairs: $M^+(SO_4^{2-})$ and $[M^+(SO_4^{2-})]_2$ (M = Na, K). *J. Phys. Chem. A* **1999**, *103*, 3423−3429.
(9) Dedonder-Lardeux, C.; Grégoire, G.; Jouvet, C.; Martrenchard, S.; Solgadi, D. Charge Separation in Molecular Clusters:Dissolution of a Salt in a Salt−$(Solvent)_n$ Cluster. *Chem. Rev.* **2000**, *100*, 4023−4038.
(10) Zhang, Q.; Carpenter, C. J.; Kemper, P. R.; Bowers, M. T. On the Dissolution Processes of Na_2I^+ and $Na_3I_2^+$ with the Association of Water Molecules: Mechanistic and Energetic Details. *J. Am. Chem. Soc.* **2003**, *125*, 3341−3352.
(11) Blades, A. T.; Peschke, M.; Verkerk, U. H.; Kebarle, P. Hydration Energies in the Gas Phase of Select $(MX)_mM^+$ Ions, Where $M^+ = Na^+, K^+, Rb^+, Cs^+, NH_4^+$ and $X^- = F^-, Cl^-, Br^-, I^-, NO_2^-, NO_3^-$. Observed Magic Numbers of $(MX)_mM^+$ Ions and Their Possible Significance. *J. Am. Chem. Soc.* **2004**, *126*, 11995−12003.
(12) Ding, C.-F.; Wang, X.-B.; Wang, L.-S. Photoelectron Spectroscopy of Doubly Charged Anions: Intramolecular Coulomb Repulsion and Solvent Stabilization. *J. Phys. Chem. A* **1998**, *102*, 8633−8636.
(13) Wang, L.-S.; Ding, C.-F.; Wang, X.-B.; Nicholas, J. B. Probing the Potential Barriers and Intramolecular Electrostatic Interactions in Free Doubly Charged Anions. *Phys. Rev. Lett.* **1998**, *81*, 2667−2670.
(14) Wang, X.-B.; Ding, C.-F.; Wang, L.-S. Photodetachment Spectroscopy of a Doubly Charged Anion: Direct Observation of the Repulsive Coulomb Barrier. *Phys. Rev. Lett.* **1998**, *81*, 3351−3354.
(15) Ding, C.-F.; Wang, X.-B.; Wang, L.-S. Photodetachment Photoelectron Spectroscopy of Doubly Charged Anions: $S_2O_8^{2-}$. *J. Chem. Phys.* **1999**, *110*, 3635−3638.
(16) Feng, Y.; Cheng, M.; Kong, X.-Y.; Xu, H.-G.; Zheng, W.-J. Microscopic Solvation of $NaBO_2$ in Water:Anion Photoelectron Spectroscopy and Ab Initio Calculations. *Phys. Chem. Chem. Phys.* **2011**, *13*, 15865−15872.
(17) Li, R.-Z.; Liu, C.-W.; Gao, Y. Q.; Jiang, H.; Xu, H.-G.; Zheng, W.-J. Microsolvation of LiI and CsI in Water: Anion Photoelectron Spectroscopy and Ab Initio Calculations. *J. Am. Chem. Soc.* **2013**, *135*, 5190−5199.
(18) Wang, X.-B.; Woo, H.-K.; Jagoda-Cwiklik, B.; Jungwirth, P.; Wang, L.-S. First Steps towards Dissolution of $NaSO_4^-$ by Water. *Phys. Chem. Chem. Phys.* **2006**, *8*, 4294−4296.
(19) Gruenloh, C. J.; Carney, J. R.; Arrington, C. A.; Zwier, T. S.; Fredericks, S. Y.; Jordan, K. D. Infrared Spectrum of a Molecular Ice Cube:The S_4 and D_{2d} Water Octamers in Benzene−$(Water)_8$. *Science* **1997**, *276*, 1678−1681.
(20) Ebata, T.; Fujii, A.; Mikami, N. Vibrational Spectroscopy of Small-Sized Hydrogen-Bonded Clusters and Their Ions. *Int. Rev. Phys. Chem.* **1998**, *17*, 331−361.
(21) Beyer, M.; Williams, E. R.; Bondybey, V. E. Unimolecular Reactions of Dihydrated Alkaline Earth Metal Dications $M^{2+}(H_2O)_2$, M = Be, Mg, Ca, Sr, and Ba: Salt-Bridge Mechanism in the Proton-Transfer Reaction $M^{2+}(H_2O)_2 \rightarrow MOH^+ + H_3O^+$. *J. Am. Chem. Soc.* **1999**, *121*, 1565−1573.
(22) Bieske, E. J.; Dopfer, O. High-Resolution Spectroscopy of Cluster Ions. *Chem. Rev.* **2000**, *100*, 3963−3998.
(23) Duncan, M. A. Frontiers in the Spectroscopy of Mass-Selected Molecular Ions. *Int. J. Mass Spectrom.* **2000**, *200*, 545−569.
(24) Robertson, E. G.; Simons, J. P. Getting into Shape: Conformational and Supramolecular Landscapes in Small Biomolecules and Their Hydrated Clusters. *Phys. Chem. Chem. Phys.* **2001**, *3*, 1−18.
(25) Duncan, M. A. Infrared Spectroscopy to Probe Structure and Dynamics in Metal Ion−Molecule Complexes. *Int. Rev. Phys. Chem.* **2003**, *22*, 407−435.
(26) Robertson, W. H.; Johnson, M. A. Molecular Aspects of Halide Ion Hydration: The Cluster Approach. *Annu. Rev. Phys. Chem.* **2003**, *54*, 173−213.
(27) Kamariotis, A.; Boyarkin, O. V.; Mercier, S. R.; Beck, R. D.; Bush, M. F.; Williams, E. R.; Rizzo, T. R. Infrared Spectroscopy of Hydrated Amino Acids in the Gas Phase: Protonated and Lithiated Valine. *J. Am. Chem. Soc.* **2005**, *128*, 905−916.
(28) Lisy, J. M. Infrared Studies of Ionic Clusters: The Influence of Yuan T. Lee. *J. Chem. Phys.* **2006**, *125*, 132302/1−132302/19.
(29) Asmis, K. R.; Neumark, D. M. Vibrational Spectroscopy of Microhydrated Conjugate Base Anions. *Acc. Chem. Res.* **2011**, *45*, 43−52.
(30) Jiang, L.; Wende, T.; Bergmann, R.; Meijer, G.; Asmis, K. R. Gas-Phase Vibrational Spectroscopy of Microhydrated Magnesium Nitrate Ions $[MgNO_3(H_2O)_{1-4}]^+$. *J. Am. Chem. Soc.* **2010**, *132*, 7398−7404.
(31) Bush, M. F.; Saykally, R. J.; Williams, E. R. Evidence for Water Rings in the Hexahydrated Sulfate Dianion from IR Spectroscopy. *J. Am. Chem. Soc.* **2007**, *129*, 2220−2221.
(32) Merrick, J. P.; Moran, D.; Radom, L. An Evaluation of Harmonic Vibrational Frequency Scale Factors. *J. Phys. Chem. A* **2007**, *111*, 11683−11700.
(33) Yacovitch, T. I.; Wende, T.; Jiang, L.; Heine, N.; Meijer, G.; Neumark, D. M.; Asmis, K. R. Infrared Spectroscopy of Hydrated Bisulfate Anion Clusters: $HSO_4^-(H_2O)_{1-16}$. *J. Phys. Chem. Lett.* **2011**, *2*, 2135−2140.
(34) Jiang, L.; Sun, S.-T.; Heine, N.; Liu, J.-W.; Yacovitch, T. I.; Wende, T.; Liu, Z.-F.; Neumark, D. M.; Asmis, K. R. Large Amplitude Motion in Cold Monohydrated Dihydrogen Phosphate Anions H_2PO_4−(H_2O): Infrared Photodissociation Spectroscopy Combined with Ab Initio Molecular Dynamics Simulations. *Phys. Chem. Chem. Phys.* **2014**, *16*, 1314−1318.
(35) Moran, A.; Mukamel, S. The Origin of Vibrational Mode Couplings in Various Secondary Structural Motifs of Polypeptides. *Proc. Natl. Acad. Sci. U.S.A.* **2004**, *101*, 506−510.
(36) Guo, R.; Mukamel, S.; Klug, D. R. Geometry Determination of Complexes in a Molecular Liquid Mixture Using Electron-Vibration−Vibration Two-Dimensional Infrared Spectroscopy with a Vibrational Transition Density Cube Method. *Phys. Chem. Chem. Phys.* **2012**, *14*, 14023−14033.